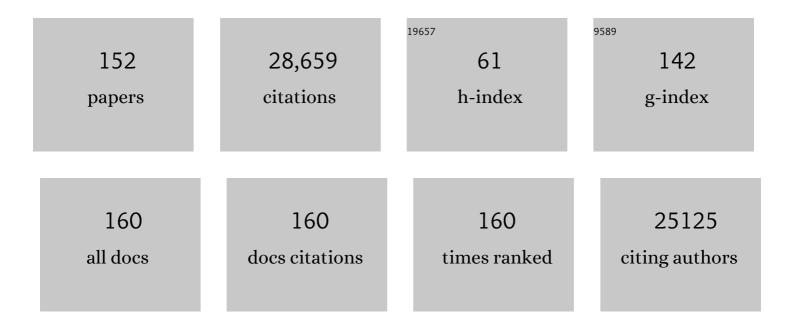
List of Publications by Year in descending order

Source: https://exaly.com/author-pdf/1902952/publications.pdf Version: 2024-02-01



#	Article	IF	CITATIONS
1	Solar Water Splitting Cells. Chemical Reviews, 2010, 110, 6446-6473.	47.7	8,307
2	Nickel–Iron Oxyhydroxide Oxygen-Evolution Electrocatalysts: The Role of Intentional and Incidental Iron Incorporation. Journal of the American Chemical Society, 2014, 136, 6744-6753.	13.7	2,659
3	Cobalt–Iron (Oxy)hydroxide Oxygen Evolution Electrocatalysts: The Role of Structure and Composition on Activity, Stability, and Mechanism. Journal of the American Chemical Society, 2015, 137, 3638-3648.	13.7	1,587
4	Solution-Cast Metal Oxide Thin Film Electrocatalysts for Oxygen Evolution. Journal of the American Chemical Society, 2012, 134, 17253-17261.	13.7	1,403
5	Enhanced absorption and carrier collection in Si wire arrays for photovoltaic applications. Nature Materials, 2010, 9, 239-244.	27.5	1,085
6	Oxygen Evolution Reaction Electrocatalysis on Transition Metal Oxides and (Oxy)hydroxides: Activity Trends and Design Principles. Chemistry of Materials, 2015, 27, 7549-7558.	6.7	944
7	Photoelectrochemical Hydrogen Evolution Using Si Microwire Arrays. Journal of the American Chemical Society, 2011, 133, 1216-1219.	13.7	561
8	Reactive Fe-Sites in Ni/Fe (Oxy)hydroxide Are Responsible for Exceptional Oxygen Electrocatalysis Activity. Journal of the American Chemical Society, 2017, 139, 11361-11364.	13.7	532
9	Energy-Conversion Properties of Vapor-Liquid-Solid–Grown Silicon Wire-Array Photocathodes. Science, 2010, 327, 185-187.	12.6	489
10	Measurement Techniques for the Study of Thin Film Heterogeneous Water Oxidation Electrocatalysts. Chemistry of Materials, 2017, 29, 120-140.	6.7	473
11	Evaluation of Pt, Ni, and Ni–Mo electrocatalysts for hydrogen evolution on crystalline Si electrodes. Energy and Environmental Science, 2011, 4, 3573.	30.8	440
12	Adaptive semiconductor/electrocatalyst junctions in water-splitting photoanodes. Nature Materials, 2014, 13, 81-86.	27.5	418
13	Revised Oxygen Evolution Reaction Activity Trends for First-Row Transition-Metal (Oxy)hydroxides in Alkaline Media. Journal of Physical Chemistry Letters, 2015, 6, 3737-3742.	4.6	417
14	Fe (Oxy)hydroxide Oxygen Evolution Reaction Electrocatalysis: Intrinsic Activity and the Roles of Electrical Conductivity, Substrate, and Dissolution. Chemistry of Materials, 2015, 27, 8011-8020.	6.7	395
15	Design of aqueous redox-enhanced electrochemical capacitors with high specific energies and slow self-discharge. Nature Communications, 2015, 6, 7818.	12.8	300
16	Semiconductor–Electrocatalyst Interfaces: Theory, Experiment, and Applications in Photoelectrochemical Water Splitting. Accounts of Chemical Research, 2016, 49, 733-740.	15.6	281
17	Pulse-Electrodeposited Ni–Fe (Oxy)hydroxide Oxygen Evolution Electrocatalysts with High Geometric and Intrinsic Activities at Large Mass Loadings. ACS Catalysis, 2015, 5, 6680-6689.	11.2	265
18	Accelerating water dissociation in bipolar membranes and for electrocatalysis. Science, 2020, 369, 1099-1103.	12.6	255

#	Article	IF	CITATIONS
19	Nanoparticle Assembly of Ordered Multicomponent Mesostructured Metal Oxides via a Versatile Solâ~'Gel Process. Chemistry of Materials, 2006, 18, 6391-6396.	6.7	232
20	Si microwire-array solar cells. Energy and Environmental Science, 2010, 3, 1037.	30.8	217
21	Effects of Intentionally Incorporated Metal Cations on the Oxygen Evolution Electrocatalytic Activity of Nickel (Oxy)hydroxide in Alkaline Media. ACS Catalysis, 2016, 6, 2416-2423.	11.2	199
22	High-performance Si microwire photovoltaics. Energy and Environmental Science, 2011, 4, 866.	30.8	196
23	Fluorination-enabled Reconstruction of NiFe Electrocatalysts for Efficient Water Oxidation. Nano Letters, 2021, 21, 492-499.	9.1	190
24	Earth-Abundant Oxygen Electrocatalysts for Alkaline Anion-Exchange-Membrane Water Electrolysis: Effects of Catalyst Conductivity and Comparison with Performance in Three-Electrode Cells. ACS Catalysis, 2019, 9, 7-15.	11.2	189
25	Precise oxygen evolution catalysts: Status and opportunities. Scripta Materialia, 2014, 74, 25-32.	5.2	165
26	Redox-Enhanced Electrochemical Capacitors: Status, Opportunity, and Best Practices for Performance Evaluation. ACS Energy Letters, 2017, 2, 2581-2590.	17.4	164
27	Potential-sensing electrochemical atomic force microscopy for in operando analysis of water-splitting catalysts and interfaces. Nature Energy, 2018, 3, 46-52.	39.5	159
28	Harnessing the Sol–Gel Process for the Assembly of Non-Silicate Mesostructured Oxide Materials. Accounts of Chemical Research, 2007, 40, 784-792.	15.6	152
29	Contributions to activity enhancement via Fe incorporation in Ni-(oxy)hydroxide/borate catalysts for near-neutral pH oxygen evolution. Chemical Communications, 2015, 51, 5261-5263.	4.1	138
30	3-D Molecular Assembly of Function in Titania-Based Composite Material Systems. Accounts of Chemical Research, 2005, 38, 263-271.	15.6	136
31	Ternary Ni-Co-Fe oxyhydroxide oxygen evolution catalysts: Intrinsic activity trends, electrical conductivity, and electronic band structure. Nano Research, 2019, 12, 2288-2295.	10.4	134
32	Operando Xâ€Ray Absorption Spectroscopy Shows Iron Oxidation Is Concurrent with Oxygen Evolution in Cobalt–Iron (Oxy)hydroxide Electrocatalysts. Angewandte Chemie - International Edition, 2018, 57, 12840-12844.	13.8	131
33	An Optocatalytic Model for Semiconductor–Catalyst Water-Splitting Photoelectrodes Based on In Situ Optical Measurements on Operational Catalysts. Journal of Physical Chemistry Letters, 2013, 4, 931-935.	4.6	130
34	Metal Oxide/(oxy)hydroxide Overlayers as Hole Collectors and Oxygen-Evolution Catalysts on Water-Splitting Photoanodes. Journal of the American Chemical Society, 2019, 141, 1394-1405.	13.7	128
35	Morphology Dynamics of Single-Layered Ni(OH) <sub>2</sub> /NiOOH Nanosheets and Subsequent Fe Incorporation Studied by <i>in Situ</i> Electrochemical Atomic Force Microscopy. Nano Letters, 2017, 17, 6922-6926.	9.1	121
36	Fundamentally Addressing Bromine Storage through Reversible Solid-State Confinement in Porous Carbon Electrodes: Design of a High-Performance Dual-Redox Electrochemical Capacitor. Journal of the American Chemical Society, 2017, 139, 9985-9993.	13.7	115

#	Article	IF	CITATIONS
37	Ag/AgCl-Loaded Ordered Mesoporous Anatase for Photocatalysis. Chemistry of Materials, 2005, 17, 1409-1415.	6.7	109
38	Nanoscale semiconductor/catalyst interfaces in photoelectrochemistry. Nature Materials, 2020, 19, 69-76.	27.5	106
39	Influence of Electrolyte Cations on Ni(Fe)OOH Catalyzed Oxygen Evolution Reaction. Chemistry of Materials, 2017, 29, 4761-4767.	6.7	105
40	Membrane Electrolyzers for Impure-Water Splitting. Joule, 2020, 4, 2549-2561.	24.0	102
41	Potential-Sensing Electrochemical AFM Shows CoPi as a Hole Collector and Oxygen Evolution Catalyst on BiVO <sub>4</sub> Water-Splitting Photoanodes. ACS Energy Letters, 2018, 3, 2286-2291.	17.4	96
42	Junction behavior of n-Si photoanodes protected by thin Ni elucidated from dual working electrode photoelectrochemistry. Energy and Environmental Science, 2017, 10, 570-579.	30.8	91
43	Tunable electronic interfaces betweenÂbulk semiconductors and ligand-stabilized nanoparticle assemblies. Nature Materials, 2007, 6, 592-596.	27.5	89
44	Theory and Simulations of Electrocatalyst-Coated Semiconductor Electrodes for Solar Water Splitting. Physical Review Letters, 2014, 112, 148304.	7.8	87
45	Flexible, Polymerâ€Supported, Si Wire Array Photoelectrodes. Advanced Materials, 2010, 22, 3277-3281.	21.0	85
46	10 â€, μ m minority-carrier diffusion lengths in Si wires synthesized by Cu-catalyzed vapor-liquid-solid growth. Applied Physics Letters, 2009, 95, .	3.3	84
47	Solution-Deposited F:SnO <sub>2</sub> /TiO <sub>2</sub> as a Base-Stable Protective Layer and Antireflective Coating for Microtextured Buried-Junction H <sub>2</sub> -evolving Si Photocathodes. ACS Applied Materials & Interfaces, 2014, 6, 22830-22837.	8.0	84
48	High Energy Density Aqueous Electrochemical Capacitors with a KI-KOH Electrolyte. ACS Applied Materials & Interfaces, 2015, 7, 19978-19985.	8.0	83
49	Efficient Charge Storage in Dual-Redox Electrochemical Capacitors through Reversible Counterion-Induced Solid Complexation. Journal of the American Chemical Society, 2016, 138, 9373-9376.	13.7	83
50	Metal–Silica Hybrid Nanostructures for Surface-Enhanced Raman Spectroscopy. Advanced Materials, 2006, 18, 2829-2832.	21.0	82
51	Bipolar membrane electrolyzers enable high single-pass CO2 electroreduction to multicarbon products. Nature Communications, 2022, 13, .	12.8	81
52	Structural Analysis of Hybrid Titania-Based Mesostructured Composites. Journal of the American Chemical Society, 2005, 127, 9721-9730.	13.7	79
53	The role of Cr doping in Ni Fe oxide/(oxy)hydroxide electrocatalysts for oxygen evolution. Electrochimica Acta, 2018, 265, 10-18.	5.2	79
54	Unique chemistries of metal-nitrate precursors to form metal-oxide thin films from solution: materials for electronic and energy applications. Journal of Materials Chemistry A, 2019, 7, 24124-24149.	10.3	78

SHANNON BOETTCHER

#	Article	IF	CITATIONS
55	In Situ Photopolymerization of Pyrrole in Mesoporous TiO <sub>2</sub> . Langmuir, 2010, 26, 5319-5322.	3.5	73
56	Potentially Confusing: Potentials in Electrochemistry. ACS Energy Letters, 2021, 6, 261-266.	17.4	73
57	Ionic Processes in Water Electrolysis: The Role of Ion-Selective Membranes. ACS Energy Letters, 2017, 2, 2625-2634.	17.4	68
58	Dye-Activated Hybrid Organic/Inorganic Mesostructured Titania Waveguides. Journal of the American Chemical Society, 2004, 126, 10826-10827.	13.7	63
59	Performance and Durability of Pure-Water-Fed Anion Exchange Membrane Electrolyzers Using Baseline Materials and Operation. ACS Applied Materials & Interfaces, 2021, 13, 51917-51924.	8.0	63
60	Integrated Reference Electrodes in Anion-Exchange-Membrane Electrolyzers: Impact of Stainless-Steel Gas-Diffusion Layers and Internal Mechanical Pressure. ACS Energy Letters, 2021, 6, 305-312.	17.4	63
61	Direct in Situ Measurement of Charge Transfer Processes During Photoelectrochemical Water Oxidation on Catalyzed Hematite. ACS Central Science, 2017, 3, 1015-1025.	11.3	61
62	Photoelectrochemical Performance of CdSe Nanorod Arrays Grown on a Transparent Conducting Substrate. Nano Letters, 2009, 9, 3262-3267.	9.1	59
63	Impact of Electrocatalyst Activity and Ion Permeability on Water-Splitting Photoanodes. Journal of Physical Chemistry Letters, 2015, 6, 2427-2433.	4.6	59
64	Electrolytic synthesis of aqueous aluminum nanoclusters and in situ characterization by femtosecond Raman spectroscopy and computations. Proceedings of the National Academy of Sciences of the United States of America, 2013, 110, 18397-18401.	7.1	58
65	Atomic force microscopy with nanoelectrode tips for high resolution electrochemical, nanoadhesion and nanoelectrical imaging. Nanotechnology, 2017, 28, 095711.	2.6	58
66	Stackable bipolar pouch cells with corrosion-resistant current collectors enable high-power aqueous electrochemical energy storage. Energy and Environmental Science, 2018, 11, 2865-2875.	30.8	58
67	Structural Evolution of Metal (Oxy)hydroxide Nanosheets during the Oxygen Evolution Reaction. ACS Applied Materials & Interfaces, 2019, 11, 5590-5594.	8.0	58
68	Field-Directed and Confined Molecular Assembly of Mesostructured Materials: Basic Principles and New Opportunities. Chemistry of Materials, 2008, 20, 909-921.	6.7	57
69	Thin Cation-Exchange Layers Enable High-Current-Density Bipolar Membrane Electrolyzers via Improved Water Transport. ACS Energy Letters, 2021, 6, 1-8.	17.4	57
70	One- and Two-Photon Induced Polymerization of Methylmethacrylate Using Colloidal CdS Semiconductor Quantum Dots. Journal of the American Chemical Society, 2008, 130, 8280-8288.	13.7	56
71	Modes of Fe Incorporation in Co–Fe (Oxy)hydroxide Oxygen Evolution Electrocatalysts. ChemSusChem, 2019, 12, 2015-2021.	6.8	55
72	pH-Independent, 520 mV Open-Circuit Voltages of Si/Methyl Viologen <sup>2+/+</sup> Contacts Through Use of Radial n <sup>+</sup> p-Si Junction Microwire Array Photoelectrodes. Journal of Physical Chemistry C, 2011, 115, 594-598.	3.1	52

#	Article	IF	CITATIONS
73	CdSe Nanorods Dominate Photocurrent of Hybrid CdSeâ^'P3HT Photovoltaic Cell. ACS Nano, 2010, 4, 6132-6136.	14.6	50
74	Aqueous Solution Processing of F-Doped SnO <sub>2</sub> Transparent Conducting Oxide Films Using a Reactive Tin(II) Hydroxide Nitrate Nanoscale Cluster. Chemistry of Materials, 2013, 25, 4080-4087.	6.7	50
75	Solar energy conversion properties and defect physics of ZnSiP <sub>2</sub> . Energy and Environmental Science, 2016, 9, 1031-1041.	30.8	49
76	Catalyst Deposition on Photoanodes: The Roles of Intrinsic Catalytic Activity, Catalyst Electrical Conductivity, and Semiconductor Morphology. ACS Energy Letters, 2018, 3, 961-969.	17.4	47
77	Heterogeneous electrocatalysis goes chemical. Nature Catalysis, 2021, 4, 4-5.	34.4	47
78	Synthesis of Rutile-Phase Sn <sub><i>x</i></sub> Ti <sub>1–<i>x</i></sub> O <sub>2</sub> Solid-Solution and (SnO <sub>2</sub> ) <sub><i>x</i></sub> /(TiO <sub>2</sub> ) <sub>1–<i>x</i></sub> Core/Shell Nanoparticles with Tunable Lattice Constants and Controlled Morphologies. Chemistry of Materials, 2011, 23, 4920-4930.	6.7	45
79	A planar-defect-driven growth mechanism of oxygen deficient tungsten oxide nanowires. Journal of Materials Chemistry A, 2014, 2, 6121-6129.	10.3	45
80	Perovskite Nanowire Extrusion. Nano Letters, 2017, 17, 6557-6563.	9.1	42
81	Low-Cost Approaches to Ill–V Semiconductor Growth for Photovoltaic Applications. ACS Energy Letters, 2017, 2, 2270-2282.	17.4	42
82	Anode Catalysts in Anionâ€Exchangeâ€Membrane Electrolysis without Supporting Electrolyte: Conductivity, Dynamics, and Ionomer Degradation. Advanced Materials, 2022, 34, .	21.0	42
83	Design principles for water dissociation catalysts in high-performance bipolar membranes. Nature Communications, 2022, 13, .	12.8	42
84	A Hybrid Redox-Supercapacitor System with Anionic Catholyte and Cationic Anolyte. Journal of the Electrochemical Society, 2014, 161, A1090-A1093.	2.9	41
85	Amorphous In–Ga–Zn Oxide Semiconducting Thin Films with High Mobility from Electrochemically Generated Aqueous Nanocluster Inks. Chemistry of Materials, 2015, 27, 5587-5596.	6.7	41
86	High-κ Lanthanum Zirconium Oxide Thin Film Dielectrics from Aqueous Solution Precursors. ACS Applied Materials & Interfaces, 2017, 9, 10897-10903.	8.0	41
87	Oxygen Electrocatalysis on Mixed-Metal Oxides/Oxyhydroxides: From Fundamentals to Membrane Electrolyzer Technology. Accounts of Materials Research, 2021, 2, 548-558.	11.7	41
88	Effects of Metal Electrode Support on the Catalytic Activity of Fe(oxy)hydroxide for the Oxygen Evolution Reaction in Alkaline Media. ChemPhysChem, 2019, 20, 3089-3095.	2.1	39
89	Collaboration and Near-Peer Mentoring as a Platform for Sustainable Science Education Outreach. Journal of Chemical Education, 2015, 92, 625-630.	2.3	35
90	Control of the pH-Dependence of the Band Edges of Si(111) Surfaces Using Mixed Methyl/Allyl Monolayers. Journal of Physical Chemistry C, 2011, 115, 8594-8601.	3.1	33

#	Article	IF	CITATIONS
91	PeakForce Scanning Electrochemical Microscopy with Nanoelectrode Probes. Microscopy Today, 2016, 24, 18-25.	0.3	32
92	Unidirectional Current in a Polyacetylene Hetero-ionic Junction. Journal of the American Chemical Society, 2004, 126, 8666-8667.	13.7	31
93	Efficient n-GaAs Photoelectrodes Grown by Close-Spaced Vapor Transport from a Solid Source. ACS Applied Materials & Interfaces, 2012, 4, 69-73.	8.0	31
94	Fabrication and Electrochemical Photovoltaic Response of CdSe Nanorod Arrays. Journal of Physical Chemistry C, 2008, 112, 8516-8520.	3.1	30
95	Doping and electronic properties of GaAs grown by close-spaced vapor transport from powder sources for scalable III–V photovoltaics. Energy and Environmental Science, 2015, 8, 278-285.	30.8	30
96	Role of Combustion Chemistry in Low-Temperature Deposition of Metal Oxide Thin Films from Solution. Chemistry of Materials, 2017, 29, 9480-9488.	6.7	30
97	Earth-abundant Cu-based chalcogenide semiconductors as photovoltaic absorbers. Journal of Materials Chemistry C, 2013, 1, 657-662.	5.5	29
98	Operando Xâ€Ray Absorption Spectroscopy Shows Iron Oxidation Is Concurrent with Oxygen Evolution in Cobalt–Iron (Oxy)hydroxide Electrocatalysts. Angewandte Chemie, 2018, 130, 13022-13026.	2.0	28
99	Three-Electrode Study of Electrochemical Ionomer Degradation Relevant to Anion-Exchange-Membrane Water Electrolyzers. ACS Applied Materials & Interfaces, 2022, 14, 18261-18274.	8.0	28
100	Domain Structures of Ni and NiFe (Oxy)Hydroxide Oxygen-Evolution Catalysts from X-ray Pair Distribution Function Analysis. Journal of Physical Chemistry C, 2017, 121, 25421-25429.	3.1	25
101	What Structural Features Make Porous Carbons Work for Redox-Enhanced Electrochemical Capacitors? A Fundamental Investigation. ACS Energy Letters, 2021, 6, 854-861.	17.4	25
102	Oxygen stays put during water oxidation. Nature Catalysis, 2018, 1, 814-815.	34.4	24
103	Aluminum Oxide Thin Films from Aqueous Solutions: Insights from Solid-State NMR and Dielectric Response. Chemistry of Materials, 2018, 30, 7456-7463.	6.7	24
104	Electrochemical Nanostructuring of n-GaAs Photoelectrodes. ACS Nano, 2013, 7, 6840-6849.	14.6	21
105	Optical response of deep defects as revealed by transient photocapacitance and photocurrent spectroscopy in CdTe/CdS solar cells. Solar Energy Materials and Solar Cells, 2014, 129, 57-63.	6.2	20
106	Amorphous Mixed-Metal Oxide Thin Films from Aqueous Solution Precursors with Near-Atomic Smoothness. Journal of the American Chemical Society, 2016, 138, 16800-16808.	13.7	20
107	Reinvigorating electrochemistry education. IScience, 2021, 24, 102481.	4.1	20
108	Synthesis, characterization and properties of Mo6S8(4-tert-butylpyridine)6 and related M6S8L6 cluster complexes (M = Mo, W). Dalton Transactions RSC, 2002, , 3096.	2.3	16

SHANNON BOETTCHER

#	Article	IF	CITATIONS
109	Minerals to Materials: Bulk Synthesis of Aqueous Aluminum Clusters and Their Use as Precursors for Metal Oxide Thin Films. Chemistry of Materials, 2017, 29, 7760-7765.	6.7	15
110	Transient photocurrents on catalyst-modified n-Si photoelectrodes: insight from dual-working electrode photoelectrochemistry. Sustainable Energy and Fuels, 2018, 2, 1995-2005.	4.9	15
111	Electrochemical synthesis of flat-[Ga <sub>13â^²x</sub> In <sub>x</sub> (μ <sub>3</sub> -OH) <sub>6</sub> (μ-OH) <sub>18</sub> (H <sub) clusters as aqueous precursors for solution-processed semiconductors. Journal of Materials Chemistry C. 2014. 2. 8492-8496.</sub) 	•2C	)/sub>2414
112	Themed issue on water splitting and photocatalysis. Journal of Materials Chemistry A, 2016, 4, 2764-2765.	10.3	14
113	NSF Program Benefits Schools in Need. Science, 2011, 332, 173-174.	12.6	13
114	Low-Temperature Steam Annealing of Metal Oxide Thin Films from Aqueous Precursors: Enhanced Counterion Removal, Resistance to Water Absorption, and Dielectric Constant. Chemistry of Materials, 2017, 29, 8531-8538.	6.7	12
115	Analysis of performance-limiting defects in pn junction GaAs solar cells grown by water-mediated close-spaced vapor transport epitaxy. Solar Energy Materials and Solar Cells, 2017, 159, 546-552.	6.2	12
116	Photoelectrochemical water splitting: silicon photocathodes for hydrogen evolution. , 2010, , .		11
117	Selective Area Epitaxy of GaAs Microstructures by Close-Spaced Vapor Transport for Solar Energy Conversion Applications. ACS Energy Letters, 2016, 1, 402-408.	17.4	11
118	Tuning Charge Transport at the Interface between Indium Phosphide and a Polypyrroleâ ^ Phosphomolybdate Hybrid through Manipulation of Electrochemical Potential. Journal of Physical Chemistry B, 2002, 106, 1622-1636.	2.6	9
119	Ionic Ligand Mediated Electrochemical Charging of Gold Nanoparticle Assemblies. Nano Letters, 2008, 8, 3404-3408.	9.1	9
120	Gallium arsenide phosphide grown by close-spaced vapor transport from mixed powder sources for low-cost III–V photovoltaic and photoelectrochemical devices. Journal of Materials Chemistry A, 2016, 4, 2909-2918.	10.3	9
121	Benchmarks and Protocols for Electrolytic, Photoelectrochemical, and Solar-Thermal Water-Splitting Technologies. ACS Energy Letters, 2020, 5, 70-71.	17.4	9
122	Purification of Residual Ni and Co Hydroxides from Feâ€Free Alkaline Electrolyte for Electrocatalysis Studies. ChemElectroChem, 2022, 9, .	3.4	9
123	Transition-Metal-Incorporated Aluminum Oxide Thin Films: Toward Electronic Structure Design in Amorphous Mixed-Metal Oxides. Journal of Physical Chemistry C, 2018, 122, 13691-13704.	3.1	8
124	Controlling Catalyst–Semiconductor Contacts: Interfacial Charge Separation in p-InP Photocathodes. ACS Energy Letters, 2022, 7, 541-549.	17.4	8
125	ACS Energy Letters: Elevating Solar Fuels and Electrocatalysis Research. ACS Energy Letters, 2016, 1, 920-921.	17.4	7
126	Tunable high-κ Zr <sub>x</sub> Al <sub>1â^'x</sub> O <sub>y</sub> thin film dielectrics from all-inorganic aqueous precursor solutions. RSC Advances, 2017, 7, 39147-39152.	3.6	7

#	Article	IF	CITATIONS
127	Homojunction GaAs solar cells grown by close space vapor transport. , 2014, , .		6
128	Arsenic antisite and oxygen incorporation trends in GaAs grown by water-mediated close-spaced vapor transport. Journal of Applied Physics, 2017, 121, 093102.	2.5	5
129	Close-spaced vapor transport reactor for III-V growth using HCl as the transport agent. Journal of Crystal Growth, 2019, 506, 147-155.	1.5	5
130	Ionic-Ligand-Mediated Electrochemical Charging of Anionic Gold Nanoparticle Films and Anionicâ~'Cationic Gold Nanoparticle Bilayers. Journal of Physical Chemistry C, 2010, 114, 4168-4178.	3.1	4
131	Towards high-efficiency GaAs thin-film solar cells grown via close space vapor transport from a solid source. , 2012, , .		4
132	Towards low-cost high-efficiency GaAs photovoltaics and photoelectrodes grown via vapor transport from a solid source. Proceedings of SPIE, 2013, , .	0.8	4
133	Advanced and In Situ Analytical Methods for Solar Fuel Materials. Topics in Current Chemistry, 2015, 371, 253-324.	4.0	4
134	Catalytic hotspots get noisy. Nature, 2017, 549, 34-35.	27.8	4
135	Hydrogen-evolution-reaction kinetics pH dependence: Is it covered?. Chem Catalysis, 2022, 2, 236-238.	6.1	4
136	Understanding Surface Reactivity of Amorphous Transition-Metal-Incorporated Aluminum Oxide Thin Films. Journal of Physical Chemistry C, 2019, 123, 27048-27054.	3.1	3
137	Characterization of Electric Double-Layer Capacitor with 0.75M NaI and 0.5 M VOSO4 Electrolyte. Journal of Electrochemical Science and Technology, 2018, 9, 20-27.	2.2	3
138	Advanced Photoelectrochemical Characterization: Principles and Applications of Dual-Working-Electrode Photoelectrochemistry. , 2016, , 323-351.		2
139	Water-Vapor-Mediated Close-Spaced Vapor Transport Growth of Epitaxial Gallium Indium Phosphide Films on Gallium Arsenide Substrates. ACS Applied Energy Materials, 2018, 1, 284-289.	5.1	2
140	Understanding methanol dissociative adsorption and oxidation on amorphous oxide films. Faraday Discussions, 2022, 236, 58-70.	3.2	2
141	Low-cost growth of IIIâ $\in$ "V layers on si using close-spaced vapor transport. , 2015, , .		1
142	Sculpting Optical Properties of Thin Film IR Filters through Nanocrystal Synthesis and Additive, Solution Processing. Chemistry of Materials, 2020, 32, 8683-8693.	6.7	1
143	Energy Spotlight. ACS Energy Letters, 2020, 5, 2739-2741.	17.4	1
144	The Calculation of Transmission Coefficients at Heterogeneous Semiconductor Interfaces: A Case Study Based on the n-InP   poly(pyrrole) Interface. Materials Research Society Symposia Proceedings, 2001, 679, 1.	0.1	0

#	Article	IF	CITATIONS
145	3-D Molecular Assembly of Function in Titania-Based Composite Material Systems. ChemInform, 2005, 36, no.	0.0	0
146	Electrocatalytic Hot Spots in San Diego. ACS Energy Letters, 2019, 4, 2489-2490.	17.4	0
147	Energy Spotlight. ACS Energy Letters, 2020, 5, 3265-3267.	17.4	0
148	Energy Spotlight. ACS Energy Letters, 2020, 5, 938-939.	17.4	0
149	Correction to "Integrated Reference Electrodes in Anion-Exchange-Membrane Electrolyzers: Impact of Stainless-Steel Gas-Diffusion Layers and Internal Mechanical Pressure― ACS Energy Letters, 2021, 6, 2238-2239.	17.4	0
150	Nanoscale Catalyst/Semiconductor Contacts in Water-Splitting Photoelectrodes. , 0, , .		0
151	Towards a Molecular Understanding of Dynamic Fe-based Oxygen Evolution Catalysts. , 0, , .		0
152	Electrochemistry-Induced Restructuring of Tin-Doped Indium Oxide Nanocrystal Films of Relevance to CO <sub>2</sub> Reduction. Journal of the Electrochemical Society, 2021, 168, 126521.	2.9	0